Journal of Hazardous Materials 182 (2010) 581–590

Contents lists available at ScienceDirect

Journal of Hazardous Materials

journal homepage: www.elsevier.com/locate/jhazmat

Metal ion adsorption using polyamine-functionalized mesoporous materials prepared from bromopropyl-functionalized mesoporous silica

Zeid A. Alothman [a,*], Allen W. Apblett [b]

[a] Department of Chemistry, College of Science Building #5, P.O. Box 2455, King Saud University, Riyadh 11451, Saudi Arabia
[b] Department of Chemistry, Oklahoma State University, 107 Physical Sciences, Stillwater, OK, USA

ARTICLE INFO

Article history:
Received 31 August 2009
Received in revised form 9 May 2010
Accepted 20 June 2010
Available online 25 June 2010

Keywords:
Mesoporous
Amine
Bromopropyl
Metal ion
OSU-6-W
NMR

ABSTRACT

Mesoporous silicas carrying di-, tri-, or penta-amine functional groups were prepared by prior functionalization of a mesoporous silica with bromopropyl-functional groups followed by nucleophilic displacement of the bromine atoms by ethylenediamine, diethylenetriamine, or tetraethylenepentamine, respectively. A synthetic method was developed that gave a starting material with very high surface coverage by the 3-brompropyl groups. Batch tests were conducted to investigate the capabilities of the prepared adsorbents for the removal of copper, zinc, and cadmium from aqueous solutions. The metal adsorption capacities for these metals were determined as a function of the polyamine group used and the total nitrogen content. The tendency to chemisorb divalent metal ions was found to follow the order: $Cu^{2+} > Zn^{2+} > Cd^{2+}$. It was found that the ethylenediamine derivative unexpectedly exhibited the highest capacities. The metal sorption by the ethylenediamine functionalized silica was found to follow first order kinetics with rate constants for Cu^{2+}, Zn^{2+} and Cd^{2+} uptake of 0.028, 0.019, and 0.014 min^{-1}, respectively. The substituted mesoporous silicas showed high resistance to leaching of the grafted polyamine groups. Copper ions that were adsorbed at the surface of the mesoporous silicas can be recovered by washing with an aqueous solution of 1.0 M HNO_3. The activities of the recovered mesoporous silicas were between 80 and 90% of the original materials.

1. Introduction

Mineral processing and metal finishing industries produce large amounts of waste effluents containing copper, nickel, cobalt, zinc, cadmium, and other harmful elements [1]. The removal of heavy metal ions from wastewater has been the subject of extensive industrial research since the toxic nature of the heavy metal ions, even low at trace levels, has been a public health problem for many years [2]. Therefore, increasing pressure from environmental authorities forces the establishment of discharge limits, which in turn, requires more effective decontamination and purification methods such as the use of porous materials to remove metal ions from aqueous solution [3]. Notably, the recovery of heavy or valuable metals from process water or wastewater can often result in considerable cost savings [4,5] due to recycling of the materials. High concentrations of heavy metal ions can be precipitated as hydroxides and removed by filtration, while low concentrations of metal ions can be removed from aqueous solutions using ion exchange resins, membranes, or adsorbents [6]. A number of adsorptive compounds are capable of capturing metal ions from aqueous solution, among which are activated charcoal and clays [7]. The inherent disadvantages of these materials are their wide distribution of pore size, heterogeneous pore structure, low selectivity for heavy metal ions, and relatively low loading capacities. In order to circumvent these limitations, some promising heavy metal adsorbents have been prepared via the immobilization of ion-chelating agents on inorganic supports [5], or via the coupling of chelating ligands to a solid support, such as inorganic oxides and organic polymers [8–10]. These adsorbents have relatively high loading capacities and the, selectivity for a targeted metal ion can be increased by the proper selection of chelating ligands. The discovery of mesoporous molecular sieves has stimulated a renewed interest in adsorbent and catalyst design, and a number of papers have been published in this area [11]. Applications of mesoporous silicas as heavy metal ion adsorbents have also been reported in the literature [8–10]. Functionalized mesoporous silica with a high density of diamino groups and well-defined mesochannels that can enhance the accessibilities of molecules is required to achieve high production when applied as a catalyst [12] and to reach high capacity and selectivity when applied as an adsorbent for harmful heavy metal cations [9,13].

This investigation has focused on the application of the functionalized silica as adsorbents for the separation and removal of pollutant metal ions. Amino-functionalized mesoporous silicas

* Corresponding author. Tel.: +966 14675999; fax: +966 14675992.
E-mail address: zaothman@ksu.edu.sa (Z.A. Alothman).

0304-3894/$ – see front matter © 2010 Elsevier B.V. All rights reserved.
doi:10.1016/j.jhazmat.2010.06.072

show notable adsorption capacities for heavy and transition metal ions from solution [12,14].

Promising sorbents can be prepared by anchoring chelating agents on mesoporous silica. In this work, immobilization of the bromopropyl-functional groups and their amine derivatives is explored. The importance of the bromopropyl-functionalized mesoporous silica results from the facile addition of nucleophiles by displacement of the terminal bromide group [15]. The aim of the present investigation was the incorporation of di-, tri-, or pentamine groups onto a modified silica gel surface and testing of the ability of this new adsorbant for removal of divalent metal ions from water.

2. Experimental

2.1. Reagents and materials

The chemicals used in this work are as follows: 3-bromopropyltrichlorosilane [$(Cl_3Si(CH_2)_3Br$) (96.0%), ethylenediamine, diethylenetriamine and tetraethylenepentamine were purchased from Aldrich and used as received. Toluene, 99.8% HPLC grade, acetone and diethyl ether were dried using anhydrous sodium sulfate for three days. Solutions of divalent metals of the appropriate concentration were prepared by dissolving the metal(II) nitrates in deionized water. Different pH ranges were prepared. Acetate solutions were prepared using hydrochloric acid/sodium acetate for pH 2–4, acetic acid/sodium acetate (buffer for pH 4–6), and acetic acid/NaOH for pH 6.5–8.0. The mesoporous silica used as the starting material (OSU-6-W) was synthesized using the procedure reported in our previously published paper [13].

2.2. Characterization of mesoporous materials

X-ray powder diffraction (XRD) patterns were obtained on a Bruker AXS D-8 Advance diffractometer using Cu K_α radiation (λ = 0.154056 nm) at 40 kV and 30 mA within the 2θ range of 1.2–10°. The samples were prepared as a thin, flat layer in a plastic holder. Data were collected with the resolution of 0.02° with step time of 8.2 s at 25 °C. The interplanar spacing (d, nm) was calculated using Bragg's equation of the formula: $d_{100} = \lambda/2 \sin\theta$, where d_{100} is the interplanar distance (nm), λ is a wavelength of Cu K_α radiation and θ is the position of the first low-angle peak (°).

The diffuse reflectance infrared Fourier transform (DRIFT) spectra were recorded on a Nicolet Magna 750 FTIR. The spectra were collected for all samples in the range from 400 to 4000 cm^{-1}. The samples were ground powders diluted with potassium bromide in an approximate ratio of 1:4.

Textural properties (surface areas, pore sizes, pore volumes, and pore size distribution) were determined at −196 °C using Brunauer–Emmett–Teller (BET) multilayer nitrogen adsorption method in a conventional volumetric technique by a Quantachrome Nova 1200 instrument and Quantachrome Autosorb-3B automated gas adsorption system. All samples were degassed for 16 h at 100–150 °C prior to adsorption. This temperature range was chosen from the TGA data in order to avoid the degradation of the immobilized surface groups or templating organic molecules while at the same time removing adsorbed gases and water. The surface area was calculated using the BET six-point surface area measurement method based on adsorption data in the partial pressure (P/P_0) range from 0.05 to 0.3 and the pore volume was determined from the amount of N_2 adsorbed at P/P_0 = ca. 0.99. The calculation of pore size was performed using the Barrett–Joyner–Halenda (BJH) method applied to the adsorption data of the N_2 sorption isotherms. Elemental analysis for C and N was used to measure the amount of functional groups in the samples and was carried out on a LECO TruSpec Carbon and Nitrogen Analyzer. Solid-state ^{13}C and ^{29}Si NMR spectra were obtained with a Chemagnetics CMX-II 300 MHZ solid-state NMR spectrometer. The experimental details for these measurements were published previously [13].Metal concentrations were measured using either by UV–Visible spectrophotometer or by inductively-coupled plasma atomic emission spectroscopy. UV–Visible spectra were recorded on a Perkin Elmer (Lambda EZ 201) spectrometer in the range from 200 to 800 nm, while the ICP analysis was performed on a Spectro CIROS ICP Spectrometer. A JEOL JXM 6400 Scanning Electron Microscope (SEM) equipped with an Evex Analytical Imaging System was used to study the morphology, shape, and size of the particles of the synthesized mesoporous materials. A JEOL JEM 100 CX II Transmission Electron Microscope (TEM) was used to study the shape, and size of the pores of the mesoporous materials. Samples for analysis were prepared by placing a small amount of the mesoporous material samples into a beam capsule. Each capsule was then filled top with Polybed 812 resin and polymerized at 60 °C for 48 h in a polymerization oven. The blocks were sectioned in thin sections of about 70 nm thickness using a Sorvall MT 5000 Ultramicrotome with a Diatome diamond knife. The sections were taken and placed on 150 mesh Formvar-coated nickel grids.

2.3. Surface derivitization of the surface of the mesoporous silica with bromopropyl groups

A solution of 50 mmol (∼13.0 ml) of 3-bromopropyltrichlorosilane was prepared in 10 ml of dry toluene under a dry atmosphere within a 50 ml round-bottom flask that was sealed with a rubber septa, under a dry atmosphere. Next, the resulting solution was added drop-wise over 30 min via a syringe to a stirred suspension of 3.0 g (∼50.0 mmol) of the activated OSU-6-W mesoporous silica in 50 ml of dry toluene in a 125 ml round-bottom flask which was also closed with rubber septa. The mixture was then stirred gently for 48 h at room temperature to ensure complete reaction. The resulting solid was recovered by filtration in a sintered funnel and washed with dry toluene (3×50 ml) to rinse away any surplus 3-bromopropyltrichlorosilane. The resulting white solid was dried at 80 °C under vacuum for 24 h to give a yield of 4.97 g. IR (cm^{-1}) (KBr): 3734 (m, sh), 3597 (m, br), 2923 (m, sh), 2852 (m, sh), 1436 (m, sh), 1346 (w), 1311 (w), 1234 (s), 1089 (s, br), 978 (m, br), 798 (m, sh), 683 (w), 574 (w), and 450 (m). Elemental analysis yielded C (11.32 wt%) and N (0.09 wt%).

In order to increase the surface coverage with bromopropyl groups, a second treatment with 3-bromopropyltrichlorosilane was used after an intermediate step in which the initial bromopropyl-derivitized silica was stirred with 50 ml of distilled water for 5 h. After filtration, washing with dry toluene and drying at 80 °C under vacuum for 24 h, the resulting hydrolyzed solid was treated with 3-bromopropyltrichlorosilane as described above. This 3-step derivitzation process gave a final yield of 5.69 g of white solid. IR (cm^{-1}) (KBr): 3562 (w, br), 3241 (s, br), 2966 (w), 2933 (s, sh), 2892 (w), 2856 (s, sh), 1455 (w), 1436 (s, sh), 1350 (w), 1303 (m), 1245 (s), 1097 (s), 1045 (m), 976 (m), 804 (m, sh), 692 (m, sh), 614 (w), 559 (w), and 468 (m). Solid-state ^{29}Si CP/MAS NMR δ (ppm) are −57.3 (T^2), −65.3 (T^3), −101.5 (Q^3), and −110.6 (Q^4). Solid-state ^{13}C CP/MAS NMR δ (ppm) are 12.0 (≡Si–CH_2–)[1], 27.2 (≡Si–CH_2–CH_2–CH_2–Br)[3], and 35.3 (≡Si–CH_2–CH_2–)[2]. Elemental analysis yielded C (14.72 wt%) and N (0.16 wt%) Scheme 1.

2.4. Preparation of mesoporous silicas with immobilized polyamine ligands

The preparation of mesoporous silica with polyamine functional groups was performed by utilizing nucleophilic displacements of

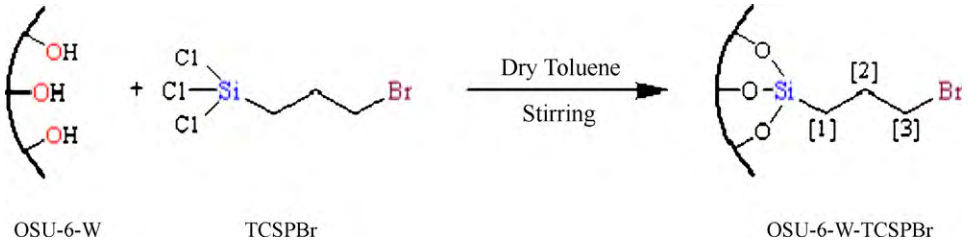

Scheme 1. Scheme to illustrate the chemical reaction involved and the number used in order to sign the carbon atom as described in the ^{13}C CP/MAS NMR.

the bromide ion from the bromopropyl-derivatized silicas. A suspension of the 1.0 g of the mesoporous silica produced via the 3-step derivitization procedure and an excess of 10 ml of target amine system (ethylenediamine, diethylenetriamine or tetraethylenepentamine) in 90 ml of dry toluene was refluxed for 48 h. The solid products were filtered, washed with successive portions of 50 ml of 0.025M NaOH, water, methanol, and then diethyl ether. The final products were dried in vacuum for 24 h. The IR spectra (KBr, cm^{-1}) of all samples showed peaks at around 1540–1640 cm^{-1} and no peaks were found due to the C-Br stretching vibration at ~ 660 cm^{-1}. Elemental analysis results are C%: 21.3, 29.67, 42.78 and N%: 19.74, 13.11, and 22.70 for the ethylenediamine, diethylenetriamine or tetraethylenepentamine derivatives, respectively.

2.5. Metal uptake experiments

The adsorption and separation experiments were conducted as follows; varying amounts of the polyamine-functionalized mesoporous silicas were shaken for 4 h with 10 ml of 100 ppm of aqueous solutions of the appropriate metal(II) ions (Cu^{2+}, Zn^{2+}, and Cd^{2+}), using 20 ml polyethylene bottles. Measurement of the metal ion concentration carried out by allowing the insoluble complex to settle down and filtering the supernatant using a 0.45 μm membrane filter syringe. The maximum metal ion uptake was calculated as mmol of M^{2+}/g ligand using the Langmuir isotherm model.

3. Results and discussion

The choices for derivitizing the surface of the mesoporous silica included silicon alkoxides, $RSi(OMe)_3$, or organosilicon halides, $RSiCl_3$, the most commonly employed silylating agents. The alkoxide reagents have lower reactivity that can lead to relatively low loading and a large number of residual silanol groups after silylation [16]. The residual silanol groups after silylation on the surface are usually considered to lead to surface hydrophilicity [17] and may have a serious effect on catalytic activity [18]. On the other hand, $RSiCl_3$ has high reactivity towards free silanol and hydrogen-bonded silanol groups [16], and results in high loading. However, difficulties can be encountered with this type of reagent due to the formation of an inhomogeneous distribution of functional groups on the surface. In particular, in the case of organically-functionalized mesoporous materials, it is difficult to control the coverage of functional groups regardless of which post-synthesis or co-condensation method that is applied [19]. Therefore, in this investigation, the chlorosilane reagent was used but a 3-step derivitization method was used to maximize the surface coverage with functional groups. The target materials were 3-halogenpropyl-functionalized mesoporous silicas that are a key intermediate for preparation of other functionalized mesoporous materials, via nucleophilic displacement of the halogen atom [20].

In the present work, the nucleophilicity of the surface silanols was enhanced by using TEA as a catalyst and employing strictly anhydrous conditions because water can interfere with the silylation reaction. Therefore, before grafting, the silica was heated at 100 °C for 2 h in order to remove the loosely bound water molecules. The reaction of 3-bromopropyltrichlorosilane to the surface silanols was enhanced by the pre-adsorption of TEA on the surface according to a literature procedure [21]. The possible interaction involved between the siliceous surface and the chlorosilanes at room temperature is hydrogen bonding, because covalent bonding ($Si_{surface}$–O–Si) would only occur above 300 °C [22]. However, it was demonstrated that, by the use of TEA, covalent bonding can be made to occur at room temperature. After the TEA adsorption, the mesoporous material was carefully washed to eliminate any TEA loosely bound to the silica surface [26]. A possible complication of the silylation reaction is competition between attach of the surface silanols on the head trichlorosilyl group and the tail bromoalkyl of the reagent. This is unlikely because the reactivity of the chlorosilanes is known to be greater than that of the bromoalkanes. Furthermore, a more reactive trichlorosilane was used rather than a monochlorosilane [24] and this was expected to exclude any possible competition [23]. In this investigation, strictly anhydrous conditions were maintained so that the trichlorosilane reacted with surface silanols without any significant polymerization [25]. FTIR spectroscopy performed after the first silanization step showed that the reaction occurred on the trichlorosilyl side of the 3-bromopropyltrichlorosilane molecules because the presence of C–Br bonds in the solid was confirmed by the presence of the absorption peak due to their stretching vibration at approximately 660 cm^{-1}. In order to increase surface coverage, a second modification step was performed after the first treating the modified sample with water in order to hydrolyze the residual silyl chloride groups that remained from the first modification step [21].

3.1. Characterization of textural properties

3.1.1. X-ray powder diffraction (XRD)

Low angle X-ray powder diffraction was performed and the results are shown in Fig. 1. The XRD of the pure mesoporous silica, OSU-6-W showed three diffraction peaks that can be indexed to a hexagonal symmetry. As already well-described in the literature [26], this symmetry indicates the ordering of cylindrical pores in a hexagonal array. The d_{100} value corresponds to the distance between two successive walls (that is, one pore diameter plus a wall thickness).

After silanization, the two functionalized samples, have smaller d spacings than the starting material. According to the average pore diameters from the surface area analysis, an average thickening of the walls occurred from 21.0 to 22.9 Å as a result of the single-silanization step and to 26.8 Å for the second silanization step. The latter result corresponds to the addition of an extra layer of Si–O–Si homogeneously spread on the original wall. It can also be noted that the d_{100} peak has become broader, indicating a slight alteration of the ordering of the mesoporous structure that likely results from inhomogenous distribution of the 3-bromopropylsilyl groups throughout the mesoporous silica. The decrease in diffraction intensities of 1 0 0, 1 1 0, and 2 0 0 reflections also indicate that any structural order of the material did not extend over a long

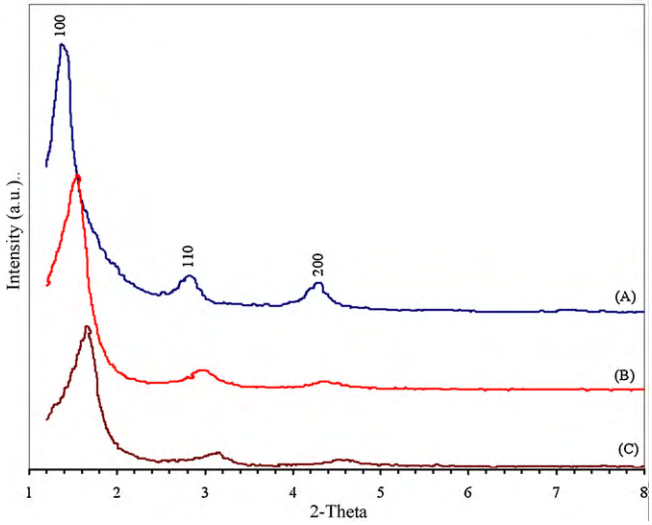

Fig. 1. Powder X-ray diffraction patterns for OSU-6-W and their bromopropylsilyl-functionalized derivatives. (A) OSU-6-W, (B) OSU-6-W-TCSPBr-1, and (C) OSU-6-W-TCSPBr-2. The spectra are shifted vertically for the sake of clarity.

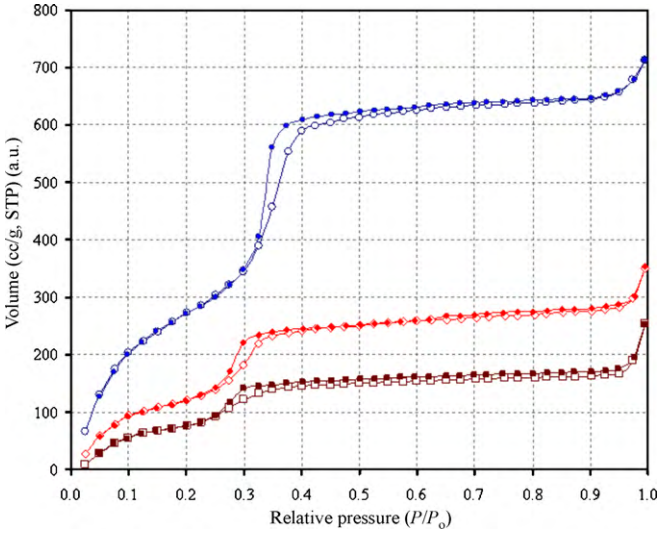

Fig. 2. Nitrogen adsorption/desorption isotherms for (○) unmodified OSU-6-W and bromopropyl-functionalized OSU-6-W; (◊) OSU-6-W-TCSPBr-1 and (□) OSU-6-W-TCSPBr-2. Open symbols: adsorption; closed symbols: desorption. The isotherm data are shifted vertically for the sake of clarity.

range, a phenomenon that is usually observed during modification of mesoporous materials [27]. It should be noted that there are no huge changes in the d_{100} spacings before and after modification which can be used as an evidence of the high chemical stability of both the parent mesoporous silica and the two modified samples.

3.1.2. Nitrogen adsorption–desorption measurements

Fig. 2 shows the nitrogen adsorption–desorption isotherms performed at 77 K of the mesoporous silicas and the textural properties are summarized in Table 1. As expected, silanization reduced the

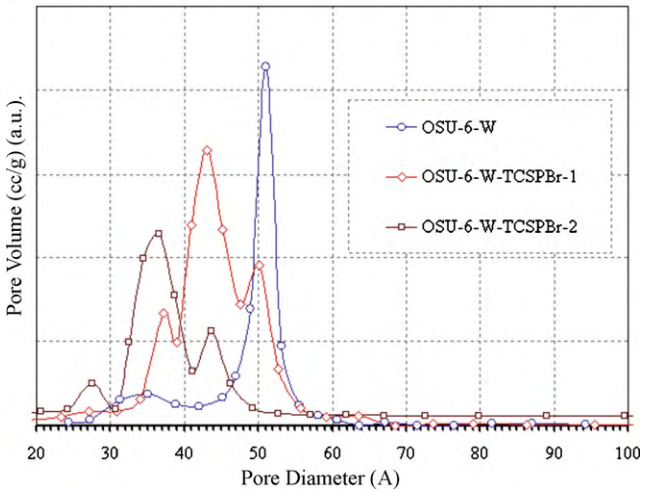

Fig. 3. The pore size distribution of (○) OSU-6-W (max. at 51.1 Å), (◊) OSU-6-W-TCSPBr-1 (max. at 43.0 Å), and (◊) OSU-6-W-TCSPBr-2 (max. at 36.5 Å).

total surface area of the mesoporous silica reduced the specific surface area (Table 1). The first silanization step reduced the surface area by 235 m^2/g while the second one reduced it by 329 m^2/g. The nitrogen uptake step that corresponds to the filling of the mesopores was shifted to lower relative pressures indicating a reduction of the pore diameter from 51.0 of the parent material to 43.0 and 36.5 Å, respectively for the silicas produced from one- and two-silanization steps (see Fig. 3). This is a direct consequence of the silanization process partially filling the pores.

3.2. Characterization of morphology

The morphology, shape, and size of the particles of the mesoporous silicas were characterized by high resolution scanning electron microscopy (SEM). The SEM micrographs of the as synthesized mesoporous silica, OSU-6 (Images A and B in Fig. 4) show that it has a narrow particle size distribution and well-defined spherical particles. These characteristics remain unchanged after the solvent-extraction step that generated the starting material used in this investigation as shown in the Fig. 4 images C and D for the mesoporous silica, OSU-6-W. The particle sizes of OSU-6 and OSU-6-W were in the range of 250–1500 nm. The unit cell parameters obtained from the transmission electron microscopy (TEM) images (Fig. 5) were close to those determined using XRD. High resolution TEM images for selected particles along [1 0 0], [1 1 1], and [1 1 0] directions correspond well with previously reported MCM-41 images.

3.3. Identification of the bromopropyl-functional groups

3.3.1. Solid-state ^{29}Si CP/MAS NMR spectroscopy

Solid-state ^{29}Si CP/MAS NMR spectra of the bromopropyl-functionalized OSU-6-W samples along with un-functionalized OSU-6-W are shown in Fig. 6. The peak around −110 ppm is assigned to the Q^4 atom $[(SiO)_4{}^*Si]$ of mesoporous silica. It is noted that there is a shoulder peak at −101.4 ppm in the solid-state ^{29}Si CP/MAS NMR spectrum of the product from the

Table 1
Textural properties determined from nitrogen adsorption–desorption experiments at 77 K and powder XRD measurements.

Sample	Specific surface area (m^2/g)	Total pore volume (cm^3/g)	Average pore size (Å)	d_{100} (Å)	Wall thickness (Å)
OSU-6-W	1283	1.24	51.1	62.4	21.0
OSU-6-W-TCSPBr-1	1048	0.94	43.0	57.1	22.9
OSU-6-W-TCSPBr-2	719	0.76	36.5	54.8	26.8

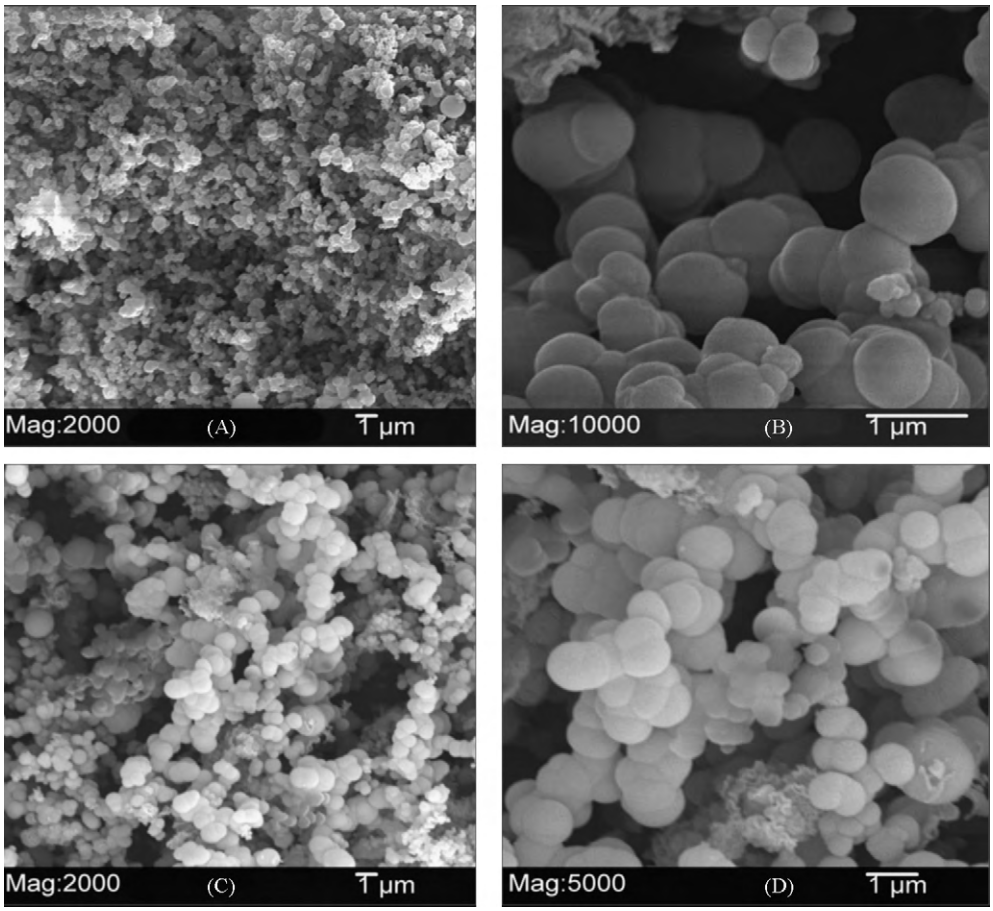

Fig. 4. SEM Images of the as-synthesized mesoporous silica OSU-6 (A and B), HCl/EtOH washed OSU-6-W (C and D).

single-silanization step that is ascribed to the Q^3 environment [$(SiO)_3{}^*SiOH$]. This peak was not observed after the second silanization step indicating that the silanol groups were almost completely silylated. In addition, the ^{29}Si resonance peak observed at approximately −65.3 ppm, due to the T^3 environment [$(SiO)_3{}^*SiR$] has the highest intensity after the second silanization step, indicating that the silyl groups were present in higher concentrations. Also the sample after the first silanization steps shows relative intensity ratios for T^1:T^2:T^3 close to 1.0:11.6:6.1 while after the second silanization step, these change to 0.0:1.0:1.6. These NMR results reveal that the silanol groups on the OSU-6-W surfaces are highly accessible to the 3-bromopropyltrichlorosilane reagent in keeping with what was observed using other silylating reagents [13].

3.3.2. Solid-state ^{13}C CP/MAS NMR spectroscopy

The presence of covalently linked organic moieties bearing bromopropylsilane chain groups in the derivitized mesoporous silicas was confirmed by ^{13}C CP/MAS solid-state NMR spectroscopy since the spectra are consistent with literature data for anchorage of bromopropylsilane chains on a silica surface [28]. The spectra (Fig. 7) show resonances at δ (ppm) values of 12.0 (≡Si–*C*H_2–), 27.2 (≡Si–CH_2–*C*H_2–*C*H_2–Br), 34.5 (≡Si–CH_2–*C*H_2–) for the single-silanization step products and δ (ppm) of 12.0 (≡Si–*C*H_2–), 27.2 (≡Si–CH_2–*C*H_2–*C*H_2–Br), and 35.3 (≡Si–CH_2–*C*H_2–) for the product from two silanization steps. Peaks corresponding to the organosiloxane moieties are relatively broad, indicating restricted mobility of the functional groups attached to the silica framework.

3.3.3. Fourier transform infrared spectroscopy (FTIR)

The vibrational spectra, Fig. 8, obtained from solid samples confirmed the success of the grafting reactions, since the observed bands are very close to those reported, when bromopropyl groups were previously incorporated into similar materials. All the spectra showed a large band around 3000–3600 cm^{-1} due to adsorbed water and, possibly, a small amount of silanol groups. The efficiency of the grafting process is demonstrated by a significant decrease in the silanol band at around 3740 cm^{-1}, with an associated increase of new bands characteristic of the immobilized bromopropyl-functional groups [29]. The FTIR spectrum of the product after the first silanization step showed peaks attributable to $\nu_{as}(CH_2)$ at 2934 cm^{-1}, $\nu_s(CH_2)$ at 2889 cm^{-1}, CH_2 scissor at 1433 cm^{-1}, and CH_2–Br stretching at 1233 and 1299 cm^{-1}. After the second silanization treatment these infrared absorption bands were observed for $\nu_{as}(CH_2)$ at 2960 cm^{-1}, $\nu_s(CH_2)$ at 2892 cm^{-1}, CH_2 scissor at 1455 cm^{-1}, and CH_2–Br stretching at 1238 and 1298 cm^{-1} [29].

3.4. Total surface loading of the bromopropyl-functional groups

The Q^2, Q^3 and Q^4 of ^{29}Si NMR resonances OSU-6-W were found at −91.2, −100.4, and −107.9 ppm, respectively (Fig. 6A). The ^{29}Si NMR spectra of the brompropyl-derivitized silica contained peaks −47.4, −56.7, −66.5, −90.5, −101.4, −108.2 ppm after the first derivitization step (Fig. 6B) and at −57.3, −65.3, −101.5, and −110.6 ppm after the second derivitization step (Fig. 6C). The relative peak areas from deconvolution of the spectra are given in Table 2. The difference in silanol concentration after sily-

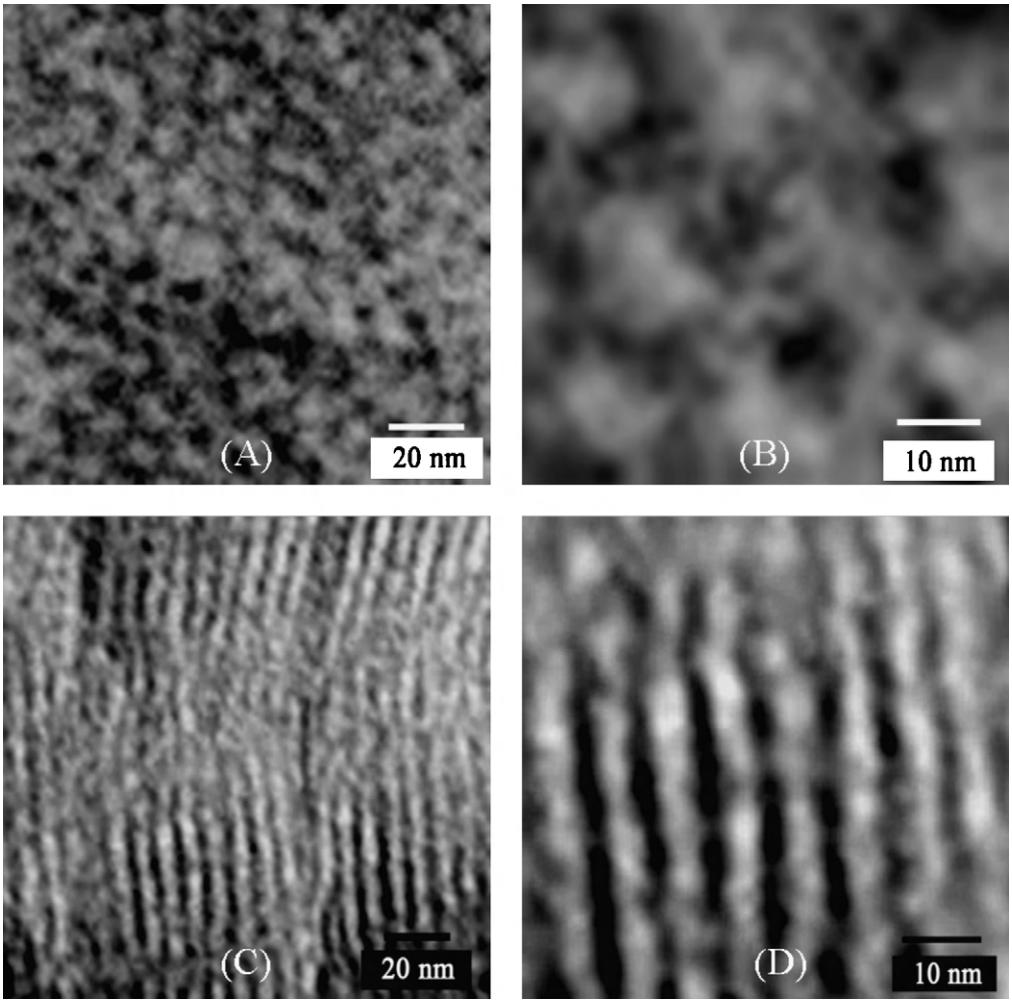

Fig. 5. Transmission electron microscopy images of OSU-6-W: (A, B) shows the hexagonal array (pore diameters ca. 50 Å) and (C, D) shows the pore diameter and wall thickness (wall thicknesses ca. 20 Å).

lation was equal to the concentration of the functional groups added.Preparation of polyamine derivitized mesoporous silicas

The immobilization of di-, tri-, and penta-amine functional groups was carried out according to a previously published method [30,33]. The reactions involved direct reaction of 3-bromopropyl-functionalized mesoporous silica with an excess of the corresponding amine ligand in the presence of triethylamine that was used to scavenge the HBr generated by the derivitization

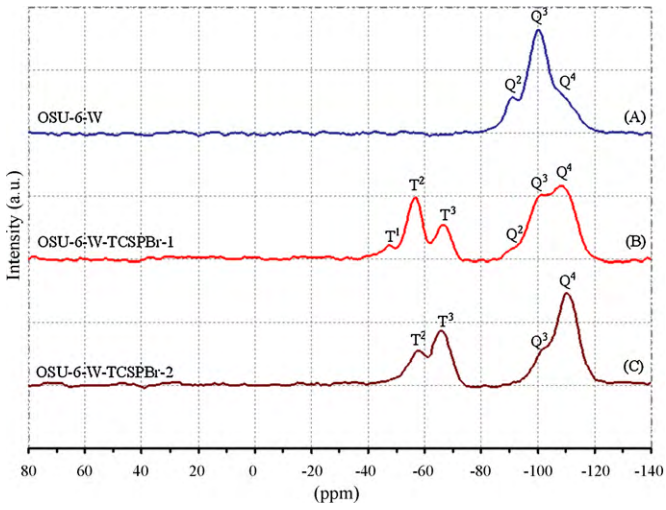

Fig. 6. Solid-state ^{29}Si NMR spectra of (A) unmodified OSU-6-W, (B) modified OSU-6-W-TCSPBr-1, and (C) the modified OSU-6-W-TCSPBr-2.

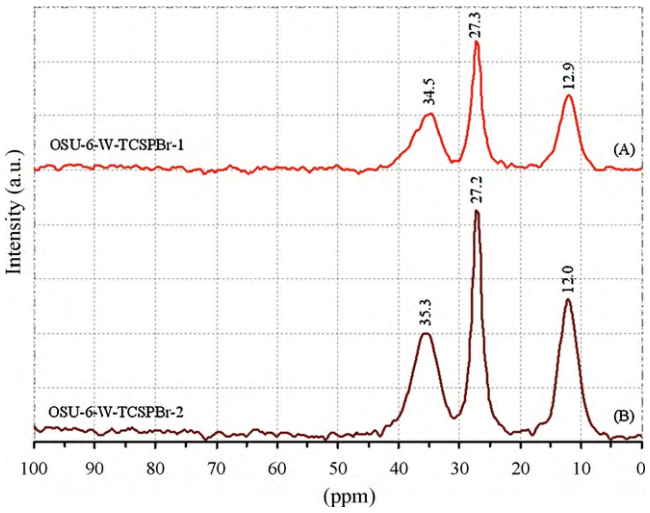

Fig. 7. Solid-state ^{13}C NMR spectra of organic monolayers on mesoporous silica, OSU-6-W, with the peak assignments. (A) OSU-6-W-TCSPBr-1 and (B) OSU-6-W-TCSPBr-2.

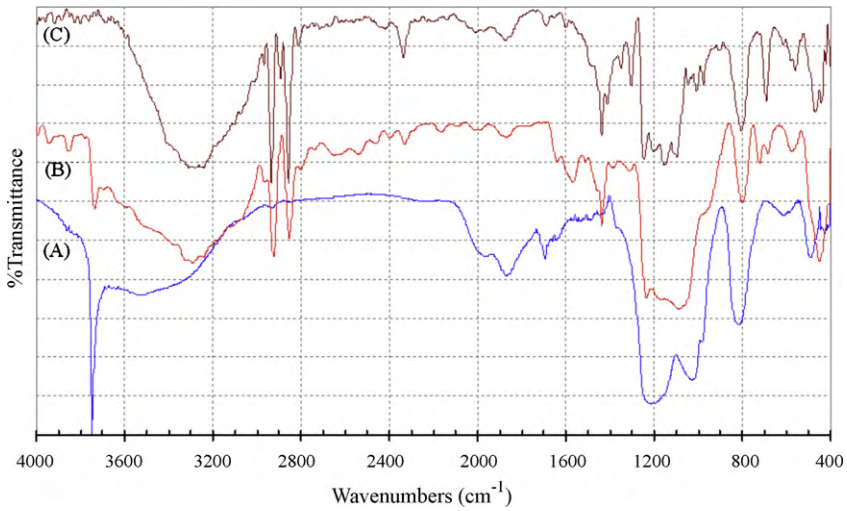

Fig. 8. Infrared spectra of (curve A) OSU-6-W, (curve B) OSU-6-W-TCSPBr-1, and (curve C) OSU-6-W-TCSPBr-2.

Table 2
Solid-state ^{29}Si CP/MAS NMR deconvolution results.

Sample	Q^4 (%)	Q^3 (%)	Q^2 (%)	[SiOH] (mmol/g)	[SiOH] (molecule/nm^2)	[TCSPBr] (group/nm^2)
OSU-6-W	14.38	71.73	13.89	14.43	6.77	–
OSU-6-W- TCSPBr-1	52.83	47.17	0.00	7.34	4.22	2.55
OSU-6-W- TCSPBr-2	81.24	18.76	0.00	3.04	2.24	4.53

reaction. The microanalytical data for the polyamine derivatives are provided in Table 3. These mesoporous inorganic–organic systems exhibit great potential in the extraction, recovery, and separation of metal ions from aqueous solution and as supported ligands for catalysis. Recently, high resolution solid-state nuclear magnetic resonance (NMR) techniques [31] and other chemical tools [17,32] have been used to examine their structural properties. Although the diamine ligand system has been known for some time and its structure is now well established [31], there is a need for studying its metal binding chemistry in some detail. In this study, several factors were investigated to optimize the metal uptake capacities of the polyamine-derivitized mesoporous silicas. These factors include exposure time, pH, and competing ions. The chemical stability of the diamine ligand system was also investigated.

3.5.1. *Identification of the immobilized di-, tri-, and penta-amine groups*

Table 3 indicates that the reaction of di-, tri-, and pent-amine with the 3-bromopropyl-functionalized mesoporous silica was nearly complete with almost all of the bromine atoms being replaced by the amine functions. The slightly lower percentages of C and N than the theoretical values may be due to polyamine groups anchoring with more than one amine group.

The FTIR spectra for the immobilized diamine ligands shows four major regions of absorption at 3500–3000, 2980–2800, 1600–1500, and 1200–900 cm^{-1} due to ν(OH) stretching, $\delta(NH_2)$ deformations, and ν(Si–O) stretching vibrations [30]. The presence of peaks in the 1600–1500 cm^{-1} region confirms the attachment of the amine groups onto the 3-bromopropyl-functionalized silica. As expected,

Table 3
Elemental analysis data for OSU-6-W-TCSPBr-2 immobilized amine ligand systems.

Immobilized sample	C%	N%	C/N
OSU-6-W-TCSPBr-2-EDA	21.31	9.74	2.19
OSU-6-W-TCSPBr-2-DETA	29.67	13.11	2.26
OSU-6-W-TCSPBr-2-TEPA	42.78	22.70	1.88

the surface areas of the mesoporous silicas decreased with increasing size of the polyamine groups, ranging from 409 m^2/g for the ethylenediamine derivative, to 357 m^2/g for the diethylentriamine derivative, and to 266 m^2/g for the tetraethylenepentamine derivative.

3.6. *Uptake capacities*

The uptake capacity of the modified mesoporous silicas with immobilized di-, tri-, and penta-amine ligand systems was investigated using varying amounts of adsorbents and one constant concentration of copper, zinc, or cadmium ions (100 ppm) at pH 5.5, 6.0, and 7.0. The results are shown in Fig. 9(a)–(c). The maximum uptakes were calculated from the Langmuir adsorption isotherms and the lists of approximate formulas for the complexes formed are listed in Table 4. Interestingly, contrary to what might be expected, derivitization with longer polyamine chains did not lead to increased capacities over that which could be achieved using ethylenediamine. It would appear that with ethylenediamine groups, the surface is already congested with adsorption sites and the addition of more groups only leads to an increase in the number of amino groups that ligate to the metal centers. The surface area measurements discussed above support the hypothesis of surface congestion since the surface areas plummet with increasing polyamine chain length. In the case of the ethylenediamine-derivitized silica, the binding of copper and zinc exceeds one metal ion per ethylenediamine group, indicating that in the presence of excess metal ions it is possible to form monoamine copper complexes that make it possible to bind up to two ions per functional group. A number of the other polyamine derivatives also bind more than one metal ion per functional group but their additional amine content makes it possible for metal chelates to form. For example the diethylentriamine derivative binds 1.5 copper ions per functional group, making it possible that two adjacent diethylentriamine groups chelate to three copper ions via two copper-amine linkages per ion. Curiously, the binding of copper to the ethylenediamine derivitized mesoporous silica exceeded the theoretical limit

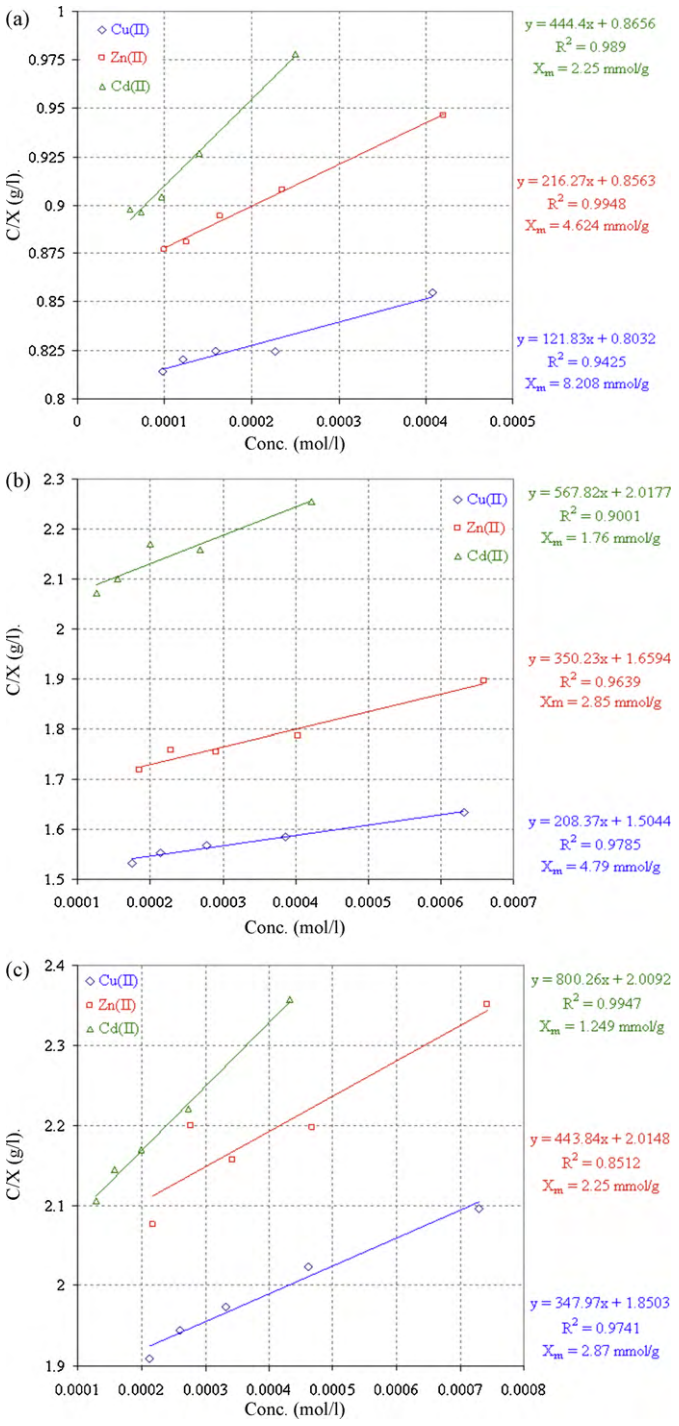

Fig. 9. (a) The langmuir adsorption isotherms of Cu^{2+}, Zn^{2+}, and Cd^{2+} ions adsorbed by OSU-6-W-TCSPBr-2-EDA adsorbent. (b) The langmuir adsorption isotherms of Cu^{2+}, Zn^{2+}, and Cd^{2+} ions adsorbed by OSU-6-W-TCSPBr-2-DETA adsorbent. (c) The langmuir adsorption isotherms of Cu^{2+}, Zn^{2+}, and Cd^{2+} ions adsorbed by OSU-6-W-TCSPBr-2-TEPA adsorbent.

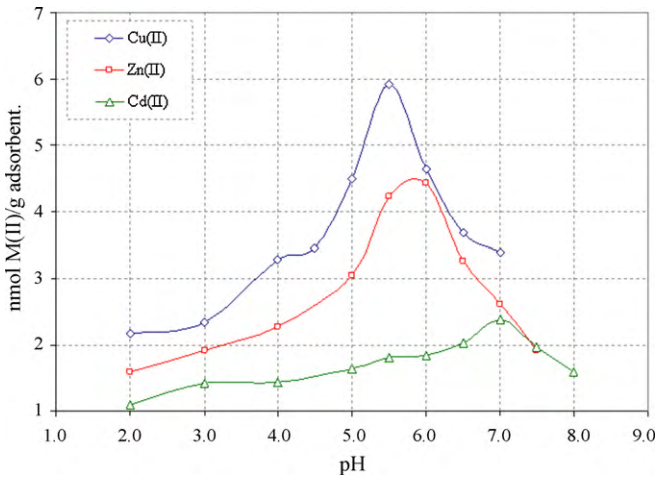

Fig. 10. Metal uptake versus pH (pH 2–8, HCl/acetate solution, 4 h shaking time) using OSU-6-W-TCSPBr-2-EDA.

of two copper ions per ethylenediamine group. It is possible that this was the result of the binding of copper clusters through the intermediacy of bridging ligands such as acetate from the buffer, the formation of an electrochemical double layer, or binding of copper ions to other parts of the derivitized silica. Future work is necessary to determine which of these mechanisms is correct.

3.7. Effect of pH

The effect of changing the solution pH on the uptake of copper, zinc, and cadmium ions is shown in Fig. 10. The results show an increase of metal ion uptake with increasing pH value reaching a maximum at pH 5.5 in the case of copper, at pH 6.0 for zinc, and at pH 7.0 in the case of cadmium. Lower uptake occurs at lower pH values due to the protonation of the amine moieties [33].

3.8. Effect of exposure time

The rate of uptake of the metal ions (Cu^{2+}, Zn^{2+}, and Cd^{2+}) as mmol M^{2+} per gram of ethylenediamine functionalized silica versus time was determined by shaking the adsorbant with an aqueous solution of the divalent metal ion at different time intervals (Fig. 11). It was found that the metal ion uptake increased as a function of exposure time in a nonlinear fashion. The adsorption rate was found to be first order and the rate constants for the adsorption for the three metal ions, Cu^{2+}, Zn^{2+}, and Cd^{2+}, were 0.028, 0.019, and 0.014 min^{-1}, respectively. These rates are faster than those reported by El Nahhal et al. [32] for a similar mesoporous silica derivative, a phenomenon that can be attributed to the higher surface area and larger pore size of the material used in this investigation.

3.9. Effect of competing ions

The uptake of a mixture of all three metal ions (copper, zinc, and cadmium at 0.05 mmol each) by 1.0 g of the ethylenedi-

Table 4
The uptake capacities from the Langmuir adsorption isotherms and the approximate formulas for the complexes formed.

Adsorbent	Uptake capacity (mg/g)			[group] (mmol/g)	Group: metal ion		
	Cu^{2+}	Zn^{2+}	Cd^{2+}		Cu^{2+}	Zn^{2+}	Cd^{2+}
OSU-6-W-TCSPBr-2-EDA	522	302	253	3.38	(2:5)	(3:4)	(3:2)
OSU-6-W-TCSPBr-2-DETA	304	186	198	3.12	(2:3)	(1:1)	(2:1)
OSU-6-W-TCSPBr-2-TEPA	182	147	141	3.24	(1:1)	(3:2)	(2:1)

Table 5
Distribution coefficient (K_d) of mesoporous-immobilized diamine for a mixture of metal ions[a] [K_d is defined as the amount of adsorbed metal (in μg) on 1.0 g of adsorbing material divided by the metal concentration (in μg/ml) remaining in the treated waste stream].

pH	Cu^{2+}		Zn^{2+}		Cd^{2+}		$Cu^{2+} + Zn^{2+} + Cd^{2+}$
	a	b	a	b	a	b	
5.5	435,000	382,800	365,400	278,400	208,800	147,900	809,100
6.0	400,200	313,200	435,000	339,300	321,900	217,500	870,000
7.0	287,100	200,100	339,300	304,500	426,300	252,300	756,900

a: the uptake of metal ion when exist alone; b: the uptake of metal ion from mixture of competing ions.
[a] 0.05 mmol of each metal ion was used.

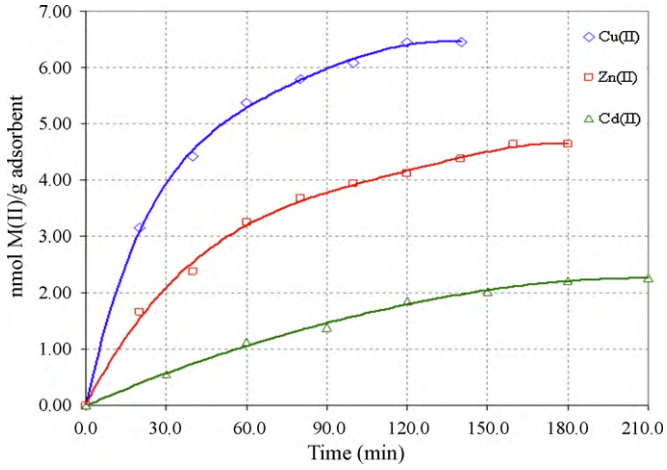

Fig. 11. The uptake of Cu^{2+}, Zn^{2+}, and Cd^{2+} ions by the mesoporous immobilized diamine ligand system versus time.

amine functionalized mesoporous silica was studied at different pH values. Maximum uptakes for copper, zinc, and cadmium ions were achieved at their optimum pH values (Table 5). For example, at pH 5.5, the uptake capacity is in the order: copper > zinc > cadmium, whereas at pH 6.0, the uptake is in the order of zinc > copper > cadmium and at pH 7.0 the order of uptake is zinc > cadmium > copper. Overall, the presence of competing ions does not affect to a major degree the uptake of zinc or copper but the uptake of cadmium is severely inhibited by the competing ions. This may be due to lower stability of the cadmium complexes compared to the other metal ions. The distribution coefficients, K_d, for the binding of the transition metal ions tested in this investigation were found be as high as 435,000 ml/g (Table 5). [K_d is defined as the amount of adsorbed metal (in μg) on 1.0 g of adsorbing material divided by the metal concentration (in μg/ml) remaining in the treated waste stream.]

3.10. Regeneration of the absorbent

Treatment of the copper-loaded material three times with a stirred aqueous solution of 2.0M HCl for 1 h resulted in removal of the bound Cu^{2+} from the structure, regenerating the adsorbent for further metal ion uptake. The regenerated material shows decrease in the Cu^{2+} ion uptake capacity down to ~70% after the fourth regeneration. The decreases may be due to loss of the immobilized groups with washing or a strong interaction of some of the Cu^{2+} ions with the amine groups so that it cannot be released with HCl washing. The latter, will lead to blocking of the available sites for chelating. Overall, this material shows excellent regeneration.

4. Conclusion

The synthesis of 3-bromopropyl-functionalized mesoporous silicas provides a convenient intermediate for facile synthesis of mesoporous silicas with a large range of organic functionalization. The 3-step synthetic method developed in this study for this material resulting in very high loading with 3-bromopropyl groups. The resulting material has a relatively well-ordered structure with high surface areas. The average pore diameters are in the range of mesoporous materials, thus permitting size selectivity for large molecules. Mesoporous silicas carrying di-, tri- and penta-amine functional groups were successfully prepared by nucelophilic displacement of the bromine ions by ethylenediamine, diethylenetriamine, and tetraethylenepentamine, respectively. These ligand systems exhibit a high potential for separation and preconcentration of divalent metal ions Cu^{2+}, Zn^{2+}, and Cd^{2+}. The tendency to chemisorb these ions onto these functionalized systems at the optimum conditions was found in the order $Cu^{2+} > Zn^{2+} > Cd^{2+}$. The uptake capacities for these ions exceeded that reported previously for related polyamine-functionalized mesoporous silicas. This is due to the fact that the materials produced in this investigation contained more functional groups on the surface than the previously reported materials including monoamine ligand systems [30].

Acknowledgements

The author would like to thank OSU and KSU for financial support and use of some measurement facilities.

References

[1] A. Adjemian, Hydrometallurgy'94, Chapman & Hall, Cambridge, UK, 1994, pp. 3–11.
[2] G.R. Choppin, Utility of oxidation state analogs in the study of plutonium behaviour, Radiochim. Acta 859 (1999) 89–96.
[3] G. Sheng, J. Hu, X. Wang, Sorption properties of Th(IV) on the raw diatomite—effects of contact time, pH, ionic strength and temperature, Appl. Radiat. Isot. 66 (2008) 1313–1320.
[4] P. Sharma, R. Tomar, Synthesis and application of an analogue of mesolite for the removal of uranium(VI), thorium(IV), and europium(III) from aqueous waste, Micropor. Mesopor. Mater. 116 (2008) 641–652.
[5] D. Karadag, Y. Koc, M. Turan, M. Ozturk, A comparative study of linear and non-linear regression analysis for ammonium exchange by clinoptilolite zeolite, J. Hazard. Mater. 144 (2007) 432437.
[6] J.S. Kim, Ph.D. Dissertation, Seoul National University, Seoul, 1999, pp. 1–19.
[7] D.L. Guerra, R.R. Viana, C. Airoldi, Adsorption of thorium cation on modified clays MTTZ derivative, J. Hazard. Mater. (2008), doi:10.1016/j.jhazmat.2009.03.034.
[8] J. Liu, X. Feng, G.E. Fryxell, L.-Q. Wang, A.Y. Kim, M. Gong, Hybrid mesoporous materials with functionalized monolayers, Adv. Mater. 10 (1998) 161–165.
[9] X. Feng, G.E. Fryxell, L.-Q. Wang, A.Y. Kim, J. Liu, K.M. Kemner, Functionalized monolayers on ordered mesoporous supports, Science 276 (1997) 923–926.
[10] J. Brown, R. Richer, L. Mercier, One-step synthesis of high capacity mesoporous Hg^{2+} adsorbents by non-ionic surfactant assembly, Micropor. Mesopor. Mater. 37 (2000) 41–48.
[11] K.F. Lam, K.L. Yeung, G. McKay, A new approach for Cd^{2+} and Ni^{2+} removal and recovery using mesoporous adsorbent with tunable selectivity, Environ. Sci. Technol. 41 (2007) 3329–3334.
[12] B.M. Choudary, M.L. Kantam, P. Sreekanth, T. Bandopadhyay, F. Figueras, A. Tuel, Knoevenagel and Aldol Condensations catalyzed by a new diamino-functionalized mesoporous material, J. Mol. Catal. A 142 (1999) 361–365.
[13] Z.A. Othman, A.W. Apblett, Synthesis of mesoporous silica grafted with 3-glycidoxypropyltrimethoxy-silane, Mater. Lett. 63 (2009) 2331–2334.
[14] K.C. Vrancken, K. Possemiers, P. Van Der Voort, E.F. Vansant, Surface modification of silica gels with aminoorganosilanes, Colloids Surf. A 98 (1995) 235–241.
[15] A.G.S. Prado, C. Airoldi, Effect of the pesticide 2,4-D on microbial activity of the soil monitored by microcalorimetry, Thermochim. Acta 349 (2000) 17–22.

[16] H. Yang, G. Zhang, X. Hong, Y. Zhu, Silylation of mesoporous silica MCM-41 with the mixture of $Cl(CH_2)3SiCl_3$ and CH_3SiCl_3: combination of adjustable grafting density and improved hydrothermal stability, Micropor. Mesopor. Mater. 68 (2004) 119–125.
[17] G.S. Caravajal, D.E. Leyden, G.R. Quinting, G.E. Maciel, Structural characterization of (3-aminopropyl)triethoxysilane-modified silicas by silicon-29 and carbon-13 nuclear magnetic resonance, Anal. Chem. 60 (1988) 1776–1786.
[18] A.C. Blanc, S. Valle, G. Renard, D. Brunel, D.J. Macquarrie, C.R. Quinn, The preparation and use of novel immobilized guanidine catalysts in base-catalyzed epoxidation and condensation reactions, Green Chem. 2 (2000) 283–288.
[19] M. Park, S. Komarneni, Stepwise functionalization of mesoporous crystalline silica materials, Micropor. Mesopor. Mater. 25 (1998) 75–80.
[20] C.E. Song, S.G. Lee, Supported chiral catalysts on inorganic materials, Chem. Rev. 102 (2002) 3495–3524.
[21] Y. Wang, Surface modification of silicate substrates, Ph.D. Dissertation, The Graduate Faculty of the University of Akron, Akron, 2006, pp. 82–87.
[22] C.P. Tripp, M.L. Hair, Reaction of chloromethylsilanes with silica: a low-frequency infrared study, Langmuir 7 (1991) 923–927.
[23] P.G. Pape, E.P. Plueddemann, Methods for improving the performance of silane coupling agents, J. Adhes. Sci. Technol. 5 (1991) 831–842.
[24] V. Antochshuk, M. Jaroniec, Simultaneous modification of mesopores and extraction of template molecules from MCM-41 with trialkylchlorosilanes, Chem. Commun. 23 (1999) 2373–2374.
[25] R.P. Singh, J.D. Way, S.F. Dec, Silane modified inorganic membranes: effects of silane surface structure, J. Membr. Sci. 259 (2005) 34–46.
[26] C.T. Kresge, M.E. Leonowicz, W.J. Roth, J.C. Vartuli, J.S. Beck, Ordered mesoporous molecular sieves synthesized by a liquid-crystal template mechanism, Nature 359 (1992) 710–712.
[27] S. Zheng, L. Gao, L. Guo, Synthesis and characterization of copper(II)-phenanthroline complex grafted organic groups modified MCM-41, Mater. Chem. Phys. 71 (2001) 174–178.
[28] A. Cauvel, G. Renard, D. Brunel, Monoglyceride synthesis by heterogeneous catalysis using MCM-41 type silicas functionalized with amino groups, J. Org. Chem. 62 (1997) 749–751.
[29] G. Socrates, Infrared Characteristic Group Frequencies, Tables and Charts, second ed., Wiley, Chichester, 1994.
[30] F.R. Zaggout, I.M. El-Nahhal, N.M. El-Ashgar, Uptake of divalent metal ions (Cu^{2+}, Zn^{2+}, and Cd^{2+}) by polysiloxane immobilized diamine ligand system, Anal. Lett. 34 (2001) 247–266.
[31] J.J. Yang, I.M. El-Nahhal, I. Chuang, G.E. Maciel, Synthesis and solid-state NMR structural characterization of polysiloxane-immobilized amine ligands and their metal complexes, J. Non-Cryst. Solids 209 (1997) 19–39.
[32] I.M. El Nahhal, M.M. Chehimi, C. Cordier, G. Dodin, XPS NMR and FTIR structural characterization of polysiloxane-immobilized amine ligand systems, J. Non-Cryst. Solids 275 (2000) 142–146.
[33] I.M. El-Nahhal, R.V. Parish, Insoluble ligands and their applications. III. Polysiloxane diaminoethane derivatives, J. Organomet. Chem. 452 (1993) 19–22.